

Cooperative Multicell Zero-Forcing Beamforming in Cellular Downlink Channels

Oren Somekh, *Member, IEEE*, Osvaldo Simeone, *Member, IEEE*, Yeheskel Bar-Ness, *Life Fellow, IEEE*, Alexander M. Haimovich, *Senior Member, IEEE*, and Shlomo Shamai (Shitz), *Fellow, IEEE*

Abstract—In this work, a multicell cooperative zero-forcing beamforming (ZFBF) scheme combined with a simple user selection procedure is considered for the Wyner cellular downlink channel. The approach is to transmit to the user with the “best” local channel in each cell. The performance of this suboptimal scheme is investigated in terms of the conventional sum-rate scaling law and the sum-rate offset for an increasing number of users per cell. We term this characterization of the sum-rate for large number of users as *high-load regime* characterization, and point out the similarity of this approach to the standard affine approximation used in the high-signal-to-noise ratio (SNR) regime. It is shown that, under an overall power constraint, the suboptimal cooperative multicell ZFBF scheme achieves the same sum-rate growth rate and slightly degraded offset law, when compared to an optimal scheme deploying joint multicell dirty-paper coding (DPC), asymptotically with the number of users per cell. Moreover, the overall power constraint is shown to ensure in probability, equal per-cell power constraints when the number of users per-cell increases.

Index Terms—Broadcast channel, distributed antenna array, fading channels, scaling law, sum-rate capacity, Wyner cellular downlink, zero-forcing beamforming (ZFBF).

I. INTRODUCTION

THE growing demand for ubiquitous access to high-data rate services has driven researchers to consider alternative wireless communications systems for different scenarios. Cellular systems are still of major interest as the most common method for providing continuous service to mobile users, in both indoor and outdoor environments. In this context, the use of joint multicell processing has been identified as a key tool for enhancing system performance (see [1], [2] and references therein for surveys of recent results on multicell processing).

The main goal of this paper is to present and analyze efficient suboptimal scheduling schemes for the downlink channel

Manuscript received January 23, 2007; revised March 04, 2009. Current version published June 24, 2009. This work was supported by a Marie Curie Outgoing International Fellowship and the NEWCOM++ network of excellence both within the 6th and 7th European Community Framework Programmes, by the U.S. National Science Foundation under Grants ANI-03-38807 and CNS-06-25637, the REMON consortium for wireless communication, and the Israeli Science Foundation (ISF). The material in this paper was presented in part at GLOBECOM 2006, San Francisco, CA, November 2006.

O. Somekh is with the Department of Electrical Engineering, Princeton University, Princeton, NJ 08544 USA (e-mail: orens@princeton.edu).

O. Simeone, Y. Bar-Ness, and A. M. Haimovich are with the Department of Electrical and Computer Engineering, New Jersey Institute of Technology, Newark, NJ 07102 USA (e-mail: osvaldo.simeone@njit.edu; barness@njit.edu; alexander.m.haimovich@njit.edu).

S. Shamai (Shitz) is with Department of Electrical Engineering, Technion—Israel Institute of Technology, Technion City, Haifa 32000, Israel (e-mail: sshlomo@ee.technion.ac.il).

Communicated by G. Kramer, Associate Editor for Shannon Theory.

Digital Object Identifier 10.1109/TIT.2009.2021371

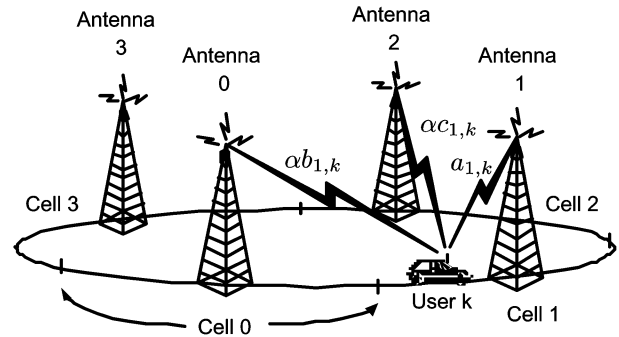


Fig. 1. Wyner's circular array system model $M = 4$.

of cellular systems that deploy multicell processing via joint zero-forcing beamforming (ZFBF). Emphasis is put on deriving analytical results that provide insight into the role of key parameters on system performance. To achieve this goal, rather than focusing on complex multicell system models as in, e.g., [3]–[5], a simple cellular model based on a model presented by Wyner in [6] is considered. According to this model (depicted in Fig. 1 with four cells), the cells are placed on a circle and each user “sees” only three cell-site antennas. In addition, the path loss is modeled by a single parameter $\alpha \in [0, 1]$ that rules inter-cell channel gains. The circular setup is homogenous and is selected to simplify the analysis. However, in the asymptotes of large number of cells, which is the regime of interest here, the circular setup and the more conventional linear setup are equivalent. Although this model is hardly realistic, it encompasses the essence of real-life system parameters, such as fading and inter-cell interference.

The downlink channel of a similar model was first considered in [7], where a suboptimal scheme based on LQ factorization of the channel matrix, an arbitrary encoding order and joint multicell dirty-paper coding (DPC), was proposed and studied. The attainable per-cell sum-rates under an overall power constraint and in the presence of Rayleigh flat fading were shown via numerical calculations to approach those of the optimal DPC scheme (with optimal encoding order), in the high-signal-to-noise ratio (SNR) region. Recently, bounds on the per-cell sum-rate capacity supported by the downlink of this model have been reported in [8], under equal per-cell power constraints, in the presence of Rayleigh flat fading. To achieve these rates, DPC techniques are deployed [9]. Unfortunately, DPC is difficult to implement in practical systems due to the high computational burden of the successive encoding involved, in particular when the number of users is large. Moreover, DPC requires accurate channel state information available at the

transmitter, which is commonly measured by the receivers and fed back to the transmitter. It is evident that for multicell processing, where many users are typically involved, these problems are particularly severe.

Linear precoding schemes that offer a tradeoff between complexity and performance have been intensively investigated in recent years, for the multiple-input multiple-output (MIMO) downlink channel [10]–[12]. A simple linear precoding scheme, which projects the multiuser channel into multiple independent single-user channels, and reduces the design into scheduling and power allocation problem, is ZFBF [13]–[15]. ZFBF is asymptotically optimal with increasing SNR, and it is easily generalized to incorporate DPC techniques [13], [16]. Recently, a ZFBF scheme has been considered in [17] for a single-cell M antennas multiple-input single-output (MISO) downlink setup under a sum-power constraint. In this suboptimal scheme, a set of (at most) M “semi-orthogonal” users to be served is selected so as to maximize the sum-rate, and independent coding is employed for each selected user. This strategy is proved to provide optimal rates (as DPC), asymptotically with the number of users K . However, determining the subset of users scheduled for transmission is a complex optimization problem, especially when K is large.

In this paper, we consider joint multicell ZFBF for the downlink of a Wyner circular setup, coupled with a simple scheduling mechanism. According to this scheme, in each cell the user with the “best” local channel (the channel from the local cell site) is scheduled for transmission. Considering at first unfaded channels, a closed-form expression for the per-cell sum-rate of the proposed scheme is derived, and is proved to hold under both overall and equal per-cell power constraints. In addition, it is shown that ZFBF scheme is superior to a simple inter-cell time sharing (ICTS) scheme, when the SNR is above a certain threshold, which increases with the inter-cell interference α . Introducing Rayleigh fading, we resort to an asymptotic analysis with an increasing number of users K (referred to as the *high-load regime*). Specifically, we formalize the *high-load regime* by following the approach of [18] and defining both the standard scaling law of the sum-rate (slope) and the corresponding offset¹. The per-cell sum-rate of ZFBF is then proved to experience the same scaling law and a slightly degraded offset when compared to an optimal DPC scheme under sum-power constraint. Moreover, it is verified that the scheme satisfies in probability the more suitable equal per-cell power constraints, asymptotically, with increasing K . Numerical results show that the asymptotic expressions derived for this setup are already valid for a modest number of users per cell. Finally, we consider a different scheduling mechanism according to which the user with the “best” total received power from the three base-stations in sight is selected for transmission. It is shown that this user selection scheme does not provide higher rates in the high-load regime.

The system model and the ZFBF scheme are described in Section II. Additional background and previous results are elaborated in Section III. The high-load regime characterization is

defined in Section IV. Sum-rate analysis for the nonfading and Rayleigh-fading setups is presented in Section V. In Section VI, an alternative user selection procedure is discussed. Numerical results and concluding remarks are presented in Sections VII and VIII, respectively. Various proofs and derivations are included in the Appendix.

II. SYSTEM MODEL

Consider a circular variant of the linear Wyner model [6] depicted in Fig. 1, in which $M > 2$ cells with K users each are arranged on a circle. Assuming a synchronous intra-cell time-division multiple-access (TDMA) scheme, according to which only one user is selected for transmission per cell, the $M \times 1$ vector baseband representation of the signals received by the *selected* users is given for an arbitrary time index by

$$\mathbf{y} = \mathbf{H}\mathbf{B}\mathbf{u} + \mathbf{z} \quad (1)$$

where \mathbf{u} is the $M \times 1$ complex Gaussian symbols vector $\mathbf{u} \sim \mathcal{CN}(\mathbf{0}, \mathbf{I}_M)$, \mathbf{B} is the beamforming $M \times M$ matrix, \mathbf{z} is the $M \times 1$ complex Gaussian additive noise vector $\mathbf{z} \sim \mathcal{CN}(\mathbf{0}, \mathbf{I}_M)$, and \mathbf{H} is the $M \times M$ channel transfer matrix, given by

$$\mathbf{H} = \begin{pmatrix} a_0 & \alpha c_0 & 0 & \cdots & 0 & \alpha b_0 \\ \alpha b_1 & a_1 & \alpha c_1 & 0 & \cdots & 0 \\ 0 & \alpha b_2 & a_2 & \alpha c_2 & \ddots & \vdots \\ \vdots & 0 & \alpha b_3 & \ddots & \ddots & 0 \\ 0 & \vdots & \ddots & \ddots & a_{M-2} & \alpha c_{M-2} \\ \alpha c_{M-1} & 0 & \cdots & 0 & \alpha b_{M-1} & a_{M-1} \end{pmatrix} \quad (2)$$

where $\alpha \in [0, 1]$ is the inter-cell interference factor representing the geometrical path losses. In addition, a_m , b_m and c_m are the flat-fading coefficients of the signals transmitted by the m th, $(m-1)$ th,² and $(m+1)$ th cell sites respectively, and received by the *selected* user of the m th cell. It is noted that the fading coefficients may be statistically dependent, depending on the users selection procedure. In addition, ergodic block-fading processes are assumed where the fade values remain constant during the TDMA slot duration. Each of the MK users perfectly measures its *own* fade coefficients $\{a_{m,k}, b_{m,k}, c_{m,k}\}$, which are fed back to the multicell transmitter via an ideal delayless feedback channel. Moreover, no user cooperation is allowed.

As mentioned earlier, the circular setup is homogenous and provides perfect symmetry between the mobiles and between the base-stations. This symmetry simplifies the analysis considerably. Moreover, in the asymptotes of large number of cells, which is the regime of interest here, the circular setup and the more conventional linear setup are equivalent; the resulting channel transfer matrices of both setups are equivalent in terms of their Frobenius norm [20].

A joint multicell ZFBF scheme is utilized, whose beamforming matrix for an arbitrary TDMA slot is given by

$$\mathbf{B} = \sqrt{\frac{MP}{\text{tr}((\mathbf{H}\mathbf{H}^\dagger)^{-1})}} \mathbf{H}^{-1} \quad (3)$$

² $\hat{n} \triangleq [n \bmod M]$.

¹This is similar to the high-SNR regime defined in [19].

where $\text{tr}(\mathbf{B}\mathbf{B}^\dagger) = MP$ is the overall average transmit power constraint, which is ensured by definition.³Substituting (3) into (1), the received signal vector reduces to

$$\mathbf{y} = \sqrt{\frac{MP}{\text{tr}((\mathbf{H}\mathbf{H}^\dagger)^{-1})}} \mathbf{u} + \mathbf{z}, \quad (4)$$

and single-user encoding–decoding schemes with long code-words lasting over many symbols (and many fading blocks) are used. Since (4) can be interpreted as a set of M identical independent parallel single-user channels, its achievable per-channel (or cell) ergodic sum–rate is given by ⁴

$$R_{\text{zfbf}} = E \left\{ \log \left(1 + \frac{MP}{\text{tr}((\mathbf{H}\mathbf{H}^\dagger)^{-1})} \right) \right\} \quad (5)$$

where the expectation is taken over the entries of \mathbf{H} . Next, expressing the trace by the nonnegative eigenvalues of $\mathbf{H}\mathbf{H}^\dagger$ in (5), recalling that the arithmetic mean of a nonnegative set is larger than its harmonic mean, and applying the Jensen’s inequality we get the following proposition, which is useful in the sequel.

Proposition 1: The achievable per-cell ergodic sum–rate of the ZFBF scheme with an arbitrary user selection procedure and total sum power constraint MP , is upper-bounded by

$$R_{\text{zfbf}} \leq \log \left(1 + \frac{P}{M} E \{ \text{tr}(\mathbf{H}\mathbf{H}^\dagger) \} \right). \quad (6)$$

Although a sum–power constraint is assumed, a more natural choice for a cellular system is to maintain per-cell power constraints. Hence, we are interested in the transmitted power of an arbitrary cell, which is averaged over the TDMA time slot duration (many symbols) and is a function of the realization of \mathbf{H}

$$P_m = [\mathbf{B}\mathbf{B}^\dagger]_{m,m} = \frac{MP [(\mathbf{H}\mathbf{H}^\dagger)^{-1}]_{m,m}}{\text{tr}((\mathbf{H}\mathbf{H}^\dagger)^{-1})}, \quad (7)$$

for $m = 0, 1, \dots, M - 1$. The following proposition will be useful later on.

Proposition 2: The average transmitted power per-cell P_m of the ZFBF scheme with an arbitrary user selection procedure (expression (7)), satisfies the following inequality :

$$P \frac{\min_n \lambda_n(\mathbf{H}\mathbf{H}^\dagger)}{\max_n \lambda_n(\mathbf{H}\mathbf{H}^\dagger)} \leq P_m \leq P \frac{\max_n \lambda_n(\mathbf{H}\mathbf{H}^\dagger)}{\min_n \lambda_n(\mathbf{H}\mathbf{H}^\dagger)}, \quad \forall m \quad (8)$$

where $\{\lambda_n(\mathbf{H}\mathbf{H}^\dagger)\}_{n=0}^{M-1}$ are the eigenvalues of $\mathbf{H}\mathbf{H}^\dagger$.

Proof: See Appendix A. \square

The above discussion holds for any ZFBF scheme with: a) sum–power constraint; b) no further power allocation via spatial “water filling;” ⁵ c) and an arbitrary selection of M users (one in each cell). In Section V, simple scheduling schemes for

both nonfading (i.e., $a_{m,k} = b_{m,k} = c_{m,k} = 1, \forall k, m$) and Rayleigh-fading (i.e., $a_{m,k}, b_{m,k}, c_{m,k} \sim \mathcal{CN}(0, 1), \forall k, m$) setups are presented and analyzed. Section III provides some additional background and related results derived for the Wyner downlink channel. These results are used as a reference for evaluating the performance of the proposed ZFBF scheme.

III. BACKGROUND

For a similar model, but with capacity-achieving joint multicell DPC scheme, the downlink per-cell ergodic sum–rate capacity with an equal per-cell power constraint P , was recently reported in [8]. The analysis considers another variant of the Wyner model referred to as the *soft-handoff model*, in which each user “sees” only two cell sites. These results can be extended to include the current circular Wyner model in a straightforward manner. Accordingly, the per-cell ergodic sum–rate capacity with an equal per-cell power constraint, for a nonfading setup, is given by

$$C_{\text{opt-nf}} \stackrel{M \rightarrow \infty}{=} \int_0^1 \log(1 + P(1 + 2\alpha \cos(2\pi\theta))^2) d\theta \quad (9)$$

and for a Rayleigh-fading setup with many users per cell ($K \gg 1$), is bounded by

$$\begin{aligned} \log(1 + P((1 - \epsilon) \log K + 1 + 2\alpha^2)) &\leq C_{\text{opt}} \\ &\leq \log(1 + (1 + 2\alpha^2)P \log K) \end{aligned} \quad (10)$$

for some $\epsilon \xrightarrow{K \rightarrow \infty} 0$.

As a reference, and assuming the system includes an even number of cells, an inter-cell time sharing (ICTS) scheduling, according to which odd and even cells are transmitting alternatively in time, can be used. This simple scheme (presented in [21] for the uplink channel) requires only limited cooperation between cells, and deploys single-user encoding–decoding schemes. Since, for each time slot, only odd or even indexed cells are transmitting, and the model assumes interference from the two adjacent cells only, inter-cell interference is avoided and the scheme demonstrates a non-interference-limited behavior. It is easily verified that the achievable per-cell ergodic sum–rate for a nonfading setup is given by

$$R_{\text{icts-nf}} = \frac{1}{2} \log(1 + 2P) \quad (11)$$

and for a Rayleigh-fading setup is well approximated (for a large number of users per cell $K \gg 1$) by

$$R_{\text{icts}} \cong \frac{1}{2} \log(1 + 2P \log K). \quad (12)$$

The latter rate is achieved by scheduling in each active cell, the user with the “best” channel for transmission.

IV. HIGH-LOAD REGIME CHARACTERIZATION

Most of the works dealing with the asymptotic analysis of downlink channels with large number of users ($K \gg 1$) are focused on the sum–rate scaling law. This traditional characterization is unable to assess the impact of other channel features, since many considered channels demonstrate the same scaling

³Later on it is argued that under certain conditions this scheme satisfies an equal per-cell average power constraints as well.

⁴A natural logarithmic base is used throughout this work.

⁵Focusing on the asymptotes of a large number of users per cell and the symmetrical nature of the model makes it unnecessary for further power allocation. However, for practical finite systems, which are asymmetric, the latter is essential for achieving good performance.

law. Moreover, a characterization based only on the scaling law does not reveal much about the actual number of users and power required to achieve a finite rate. Here, we present a more refined characterization for the scenario of large number of users (referred to as the *high-load regime*), in which the rate is expanded as an affine function of $\log \log K$. The resulting zero-order term or *high-load offset* captures the impact of other channel features, such as scheduling and coding. The high-load refinement is inspired by the seminal works of Shamai *et al.* [22] and Lozano *et al.* [19], dealing (among other things) with the power offset in the high-SNR regime. In fact, the definitions of the high-load slope and offset are similar to the respective high-SNR slope and offset, where the term $\log P$ in the latter is replaced by the term $\log K$.

In the high-load regime, the sum-rate per receive element of “good” scheduling schemes in the presence of Rayleigh fading behaves as

$$R = S_\infty (\log \log K + L_\infty) + o(1) \quad (13)$$

where S_∞ denotes the high-load slope in bits per second per hertz (bits/s/Hz)

$$S_\infty \triangleq \lim_{K \rightarrow \infty} \frac{R}{\log \log K} \quad (14)$$

and L_∞ , defined by

$$L_\infty \triangleq \lim_{K \rightarrow \infty} \left(\frac{R}{S_\infty} - \log \log K \right) \quad (15)$$

represents the high-load offset with respect to some reference channel having the same high-load slope.

Applying these definitions, we get that the high-load characterization of the optimal joint multicell DPC scheme in the presence of Rayleigh fading (expression (10)) is given by

$$S_\infty^{\text{opt}} = 1; \quad \log P \leq L_\infty^{\text{opt}} \leq \log P + \log(1 + 2\alpha^2), \quad (16)$$

while the high-load characterization of the ICTS scheme in the presence of Rayleigh fading (expression (12)) is given by

$$S_\infty^{\text{icts}} = \frac{1}{2}; \quad L_\infty^{\text{icts}} = \log P. \quad (17)$$

To conclude this section, we note that the baseline scaling law of $\log \log K$ is matched to Rayleigh-fading channels, and is motivated by the fact that the maximum of K independent and identically distributed (i.i.d.) central chi-square distributed random variables (r.v.’s) with $2n$ degrees of freedom χ_{2n}^2 , roughly behaves like $\log K$ [23 (Example 1, Appendix A)], [24]. Other fading distributions may lead to other baseline scaling laws (see, for example, [25], where a law of $\sqrt{\log K}$ is demonstrated for lognormal fading). It is also noted that, although the high-load characterization is similar to the high-SNR characterization (with $\log \log K$ takes the role of $\log P$), there is a main difference between the two asymptotic regimes. The difference lies in the fact that while the SNR is related to the input signals and additive noise vector statistics, the number of users is related to the resulting fading statistics via the user selection scheme. This fact makes the high-load parameters

hard to calculate and much more setting dependent than the general expressions derived for the high-SNR parameters [19].

V. SUM-RATE ANALYSIS

In this section, the achievable per-cell ergodic sum-rate of the ZFBF scheme is analyzed for Gaussian (i.e., nonfading) and Rayleigh block flat-fading channels, for specific user scheduling procedures. For the fading setup, we also address the high-load characterization and the implications of an increasing number of users per cell over the transmitted power of an arbitrary cell site.

A. Nonfading Setup

For nonfading channels, *round-robin* scheduling is deployed without loss of optimality. In addition, there is no need to feed back the channel coefficients since $a_{m,k} = b_{m,k} = c_{m,k} = 1$, $\forall m, k$. Hence, for each time slot, the channel transfer matrix (2) becomes circulant with $(1, \alpha, 0, \dots, 0, \alpha)$ as first row, and the following proposition holds.

Proposition 3: The per-cell average sum-rate of the ZFBF scheme is given for $\alpha < 1/2$ by

$$R_{\text{zfbf-nf}} \stackrel{M \rightarrow \infty}{=} \log \left(1 + (1 - 4\alpha^2)^{\frac{3}{2}} P \right). \quad (18)$$

This rate holds for an overall power constraint MP , and for an equal per-cell power constraints P .

Proof: See Appendix B. \square

Evidently, $R_{\text{zfbf-nf}}$ is a decreasing function of the interference factor α . Comparing (11) to (18), it is clear that the ZFBF scheme is superior to the ICTS scheme, when the SNR P is above a certain threshold

$$P_t(\alpha) = \frac{2 \left(1 - (1 - 4\alpha^2)^{\frac{3}{2}} \right)}{(1 - 4\alpha^2)^3} \quad (19)$$

which is an increasing function of α . It is noted that for $\alpha = 1/2$, the circulant channel transfer matrix \mathbf{H} is singular and channel inversion methods, such as ZFBF are not applicable. Moreover, \mathbf{H} is not guaranteed to be nonsingular for $\alpha > 0.5$ and any finite number of cells M .

B. Rayleigh-Fading Setup

For the Rayleigh-fading setup (i.e., $a_{m,k}, b_{m,k}, c_{m,k} \sim \mathcal{CN}(0, 1)$, $\forall k, m$), we propose the following strategy. For each fading block (or TDMA slot), the multicell processor selects the user with the “best” local received power (BLP) for transmission in each cell. In other words, the selected user in the m th cell is

$$\tilde{k}(m) = \underset{k}{\operatorname{argmax}} \{ |a_{m,k}|^2 \} \quad (20)$$

where $\{a_{m,k}\}_{k=1}^K$ are the fading coefficients of the m th cell transmitted signals as they are received by the m th cell users. The resulting channel transfer matrix of this suboptimal scheduling \mathbf{H} (defined in (1)) consists of diagonal entries

$a_m = a_{m,\tilde{k}(m)}$ whose amplitudes are the *maximum* of K i.i.d. chi-square distributed random variables with two degrees of freedom. The other two diagonal entries of \mathbf{H} are chi-square distributed random variables with two degrees of freedom times α .

In case \mathbf{H} is ill conditioned, the joint beamformer can start replacing the “best” users by their second “best” users until the resulting \mathbf{H} is well behaved. Since we assume that $K \gg 1$, the overall statistics is not expected to change by this user replacing procedure. The special structure of the channel transfer matrix \mathbf{H} resulting from the setup topology and the scheduling procedure plays a key role in understanding the asymptotic high-load characterization of the scheme’s per-cell sum-rate R_{zfbf} (expression (5)), which is stated in the following proposition.

Proposition 4: The high-load characterization of the ZFBF-BLP scheme is given by

$$S_{\infty}^{\text{blp}} = 1; \quad L_{\infty}^{\text{blp}} = \log P. \quad (21)$$

Proof: See Appendix C. \square

This results can be intuitively explained by the fact that due to the scheduling process, $(\mathbf{H}\mathbf{H}^\dagger)$ “becomes” diagonal ($\log K \mathbf{I}_M$) when K increases. Accordingly, for large K , $(\mathbf{H}\mathbf{H}^\dagger)^{-1}$ “behaves” like $(\mathbf{I}_M / \log K)$, and R_{zfbf} (expression (5)) is well approximated for the BLP selecting scheme by

$$R_{\text{blp}} \underset{K \gg 1}{\cong} \log(1 + P \log K). \quad (22)$$

It is concluded that the per-cell sum-rate of the ZFBF-BLP scheme scales as $\log \log K$, which is the same scaling law of the optimal multicell joint DPC scheme. Moreover, the gap between the high-load offsets of the ZFBF-BLP and that of the optimal scheme is bounded according to (16) by

$$0 \leq L_{\infty}^{\text{opt}} - L_{\infty}^{\text{blp}} \leq \log(1 + 2\alpha^2). \quad (23)$$

Hence, in the high-load regime the spectral efficiency of the ZFBF-BLP scheme is less than 1.1 [bit/s/Hz] below the rate of the optimal scheme (set $\alpha = 1$ in (23)). It is also concluded that the ZFBF-BLP scheme provides a twofold scaling law compared to the ICTS scheme (12), in the presence of Rayleigh fading. Moreover, by definition, the sum-rate of the ZFBF scheme ensures a non-interference-limited behavior for any number of users K (not necessarily large).

Finally, we consider the power constraint issue asymptotically with an increasing number of users per cell.

Proposition 5: The considered ZFBF-BLP scheme, which maintains an overall power constraint of MP , ensures in probability an equal per-cell power constraint of P , asymptotically with an increasing number of users per cell. Hence

$$P_m \xrightarrow{K \rightarrow \infty} P, \quad m = 0, 1, \dots, M-1. \quad (24)$$

Proof: See Appendix D. \square

As mentioned earlier, for cellular systems, an individual per-cell power constraint is a more reasonable choice than a sum-power constraint, which is more suitable for collocated antenna arrays.

VI. DISCUSSION

One of the reasons why the BLP user selection scheme was chosen to be the focal point of this work is that it enables analytical treatment, and specifically the derivation of a lower bound on the per-cell sum-rate in the presence of Rayleigh fading. In this section, we present a more “natural” user selection procedure referred to as best total received power (BRP), and we show that such strategy does not provide larger rates in the high-load regime. According to this scheme, in each fading block (or TDMA slot) the multicell processor selects the user with the best overall received power for transmission in each cell. In other words, the selected user in the m th cell is

$$\tilde{k}(m) = \underset{k}{\operatorname{argmax}} \left\{ |a_{m,k}|^2 + \alpha^2 (|b_{m,k}|^2 + |c_{m,k}|^2) \right\} \quad (25)$$

where $\{a_{m,k}\}_{k=1}^K$, $\{b_{m,k}\}_{k=1}^K$, and $\{c_{m,k}\}_{k=1}^K$ are the fading coefficients of the m th, $m-1$ th, and $m+1$ th cell transmitted signals, respectively, as they are received by the m th-cell users. In case \mathbf{H} is ill conditioned, the same procedure of replacing “best” users with second “best” users is deployed.

Proposition 6: The per-cell sum-rate of the ZFBF-BRP scheme is upper-bounded for any number of users per cell K by

$$R_{\text{brp}} \leq R_{\text{brp-ub}} \triangleq \log \left(1 + P \frac{\log(2K+1) + 3 \log \log K}{1 - \frac{1}{\log K}} \right). \quad (26)$$

Proof: See Appendix G. \square

Applying the definitions of the high-load slope and offset (expressions (14) and (15)) directly to the upper bound of (26) yields the following:

$$S_{\infty}^{\text{brp-ub}} = 1; \quad L_{\infty}^{\text{brp-ub}} = \log P. \quad (27)$$

Since the high-load slope and offset predicted by the upper bound equal those of the ZFBF-BPL scheme, it is concluded that the ZFBF-BRP scheme does not provide higher rates in the high-load regime than that of the ZFBF-BLP scheme. Although it is conjectured that Proposition 5 also holds for the ZFBF-BRP scheme, the issue of the individual cells’ transmitted power does not change the latter conclusion.

VII. NUMERICAL RESULTS

First, the nonfading setup is considered under the assumption that the number of cells is large $M \gg 1$ and $\alpha < 1/2$. In Fig. 2, the spectral efficiencies⁶ per cell of the optimal, ICTS, and ZFBF schemes (expressions (9), (11), and (18), respectively) are plotted as functions of the transmitted E_b/N_0 , for $\alpha = 0.4$. It is observed that the ZFBF scheme outperforms the ICTS scheme above a certain SNR threshold. The threshold $P_t(\alpha)$ (expression (19)) is shown in Fig. 3 as a function of the inter-cell interference factor α ; the ICTS scheme is superior in the region below this curve (which is a monotonically increasing

⁶The spectral efficiency $C(E_b/N_0)$ is defined through the following relations: $C(E_b/N_0) = C(\text{SNR})$ and $\text{SNR} = C(\text{SNR})E_b/N_0$.

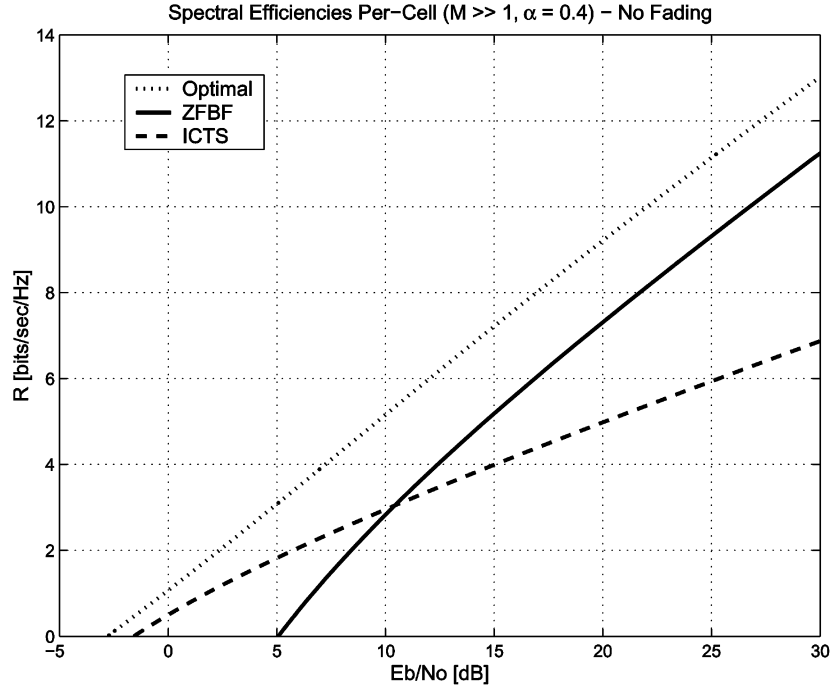


Fig. 2. Spectral efficiencies per cell with no fading versus E_b/N_0 for $\alpha = 0.4$.

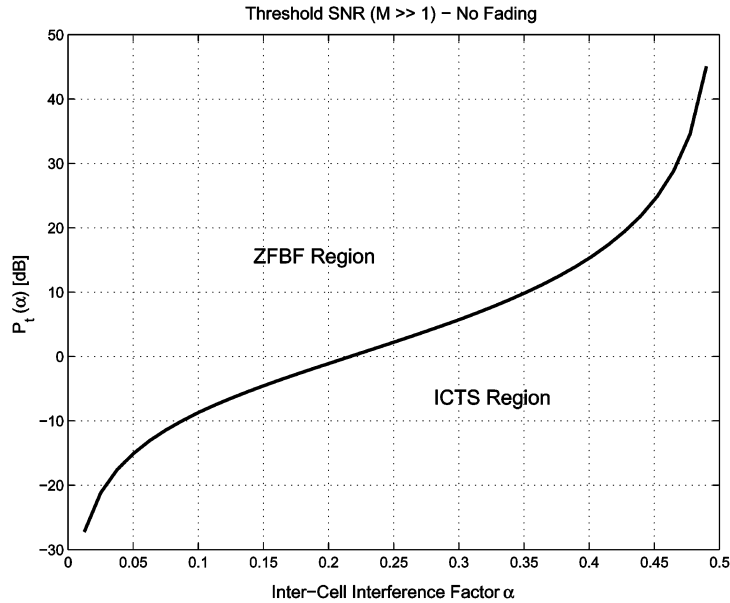


Fig. 3. The SNR threshold $P_t(\alpha)$ with no fading versus the inter-cell interference factor α .

function of α), while the ZFBF scheme prevails in the region above the curve.

Turning to the Rayleigh-fading setup, the spectral efficiencies per cell (calculated by Monte Carlo simulations) of the ICTS and ZFBF-BLP (expression (5)) schemes, and the asymptotic upper bound of the optimal scheme (expression (10)) are plotted in Fig. 4 as functions of the transmitted E_b/N_0 , for $\alpha = 0.4$, $K = 100$, and finite dimensional system of $M = 30$ cells.⁷ It is observed that for this set of parameters the ZFBF-BLP scheme loses only a fraction of a bit/s/Hz when compared to

⁷It is noted that a circular setup of $M = 30$ may be considered for any practical purpose as an infinite array [8].

the upper bound of the optimal scheme already for a modest number of users per cell (it is noted that the upper bound is valid for $K \gg 1$ and it might not be accurate for small values of K). The gap between the ZFBF-BLP curve and the per-cell sum-rate capacity upper bound is clearly explained by the fact that the ZFBF-BLP scheme does not use the distributed antenna array to enhance the reception power, but to eliminate inter-cell interference. Hence, the additional array power gain of $(1 + 2\alpha^2)$ predicted by the upper bound cannot be achieved. Moreover, for large values of E_b/N_0 , the ZFBF provides approximately twice the bits/s/Hz compared to the ICTS scheme, which can be explained by the $1/2$ high-load slope of the ICTS per-cell sum-rate expression (17).

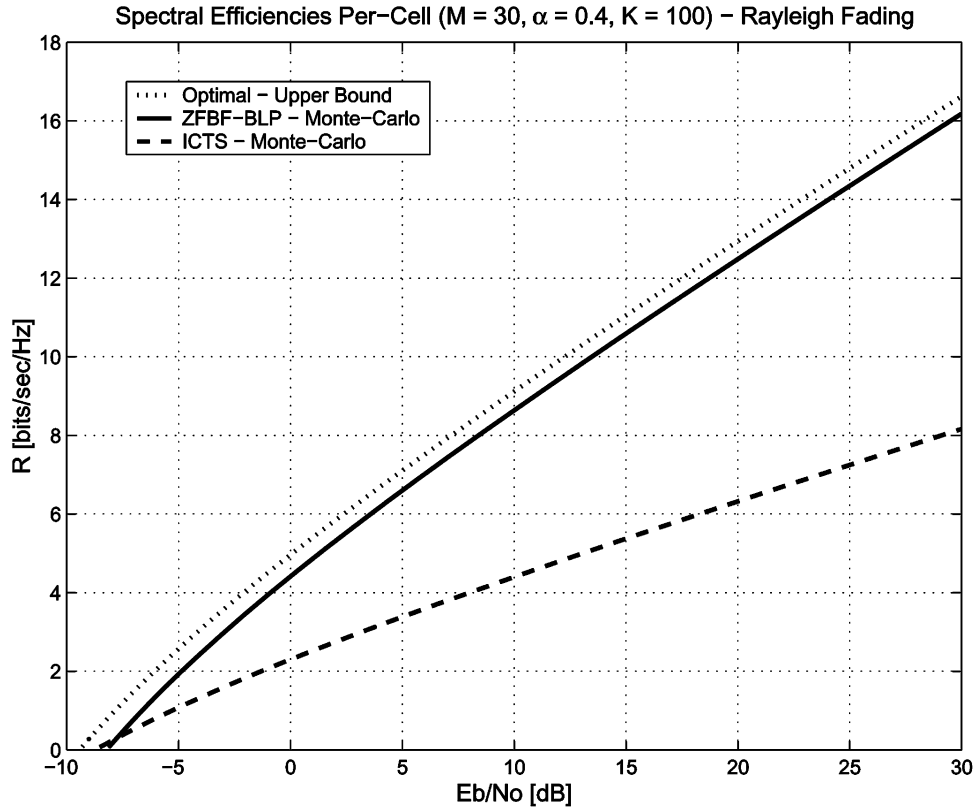


Fig. 4. Spectral efficiencies per cell in the presence of Rayleigh fading versus E_b^t/N_0 for $K = 100$, $\alpha = 0.4$, and $M = 30$.

The superiority of the ICTS scheme over the ZFBF scheme in the low-SNR regime for Gaussian channels is due to the fact that in this regime the performance is determined mainly by the average receive power (P for ICTS versus $(1 - 4\alpha^2)^{3/2}P$ for ZFBF). As the SNR increases, the $1/2$ pre-log factor of the ICTS becomes dominant and the performance of the ICTS scheme drops below that of the ZFBF scheme. For Rayleigh-fading channels and large K , this is no longer true, since the effective receive power is proportional to $\log K$. To conclude, in the low-SNR regime and Gaussian channels, ICTS is beneficial over ZFBF, while for Rayleigh-fading channels, ICTS is beneficial only when $P \log K \ll 1$ (or very low-SNR regime).

In Fig. 5, the sum-rates per cell of the ICTS and ZFBF-BLP schemes (Monte Carlo simulations, and asymptotic expressions (22) and (12)), the ZFBF-BRP (Monte Carlo simulation), and the upper bound of the optimal scheme, are plotted as functions of the number of users per-cell for $P = 10$ [dB], $\alpha = 0.4$ and $M = 30$. Examining the curves, the observations made for Fig. 4 are strengthened, since the small loss suffered by the ZFBF scheme when compared to the upper bound is demonstrated to hold over a wide range of K values. A good match between the ZFBF-BLP Monte Carlo simulation results to its asymptotic curve is observed as well, already for a modest number of users per cell. Another observation is that the BRP scheduling does not provide higher rates than the BLP scheduling, demonstrating that the claim of Proposition 4 is also valid for a modest number of users per cell.

In Fig. 6, the empirical cumulative distribution function (CDF) of an arbitrary cell normalized transmit power P_m/P is plotted for several values of the number of users per cell K and

$P = 10$ [dB]. The curves, derived by Monte Carlo simulation, demonstrate the convergence of P_m to P as predicted by Proposition 5; the probability of P_m to be in the range of $P \pm 1$ [dB] increases from 0.4 to 0.84, while the number of users increases from $K = 10$ to $K = 1000$.

VIII. CONCLUDING REMARKS

In this work, cooperative multicell ZFBF for the down-link of the circular Wyner model is studied for Gaussian and flat Rayleigh-fading channels. For the nonfading setup and round-robin scheduling, a closed-form expression for the achievable per-cell sum-rate (under both overall and equal per-cell power constraints) is derived. ZFBF is shown to demonstrate superior performance over the ICTS (i.e., frequency reuse) when the SNR crosses a certain threshold, which increases with the inter-cell interference power level (increasing α). To address the analysis in the presence of Rayleigh fading, we introduce the high-load characterization of the sum-rate, which consists of the slope and offset parameters describing the sum-rate scaling with the number of users. We propose a simple scheduling scheme, whereby in each cell the user with BLP is selected. The per-cell sum-rate of the proposed ZFBF-BLP scheme is proved to demonstrate the same growth rate of $\log \log K$ and a slightly degraded offset when compared to the optimal DPC scheme, asymptotically with an increasing number of users per cell K , while satisfying (in probability) equal per-cell power constraints. We also show that the alternative ZFBF-BRP scheme does not provide better rates in the high-load regime. Furthermore, numerical results derived by

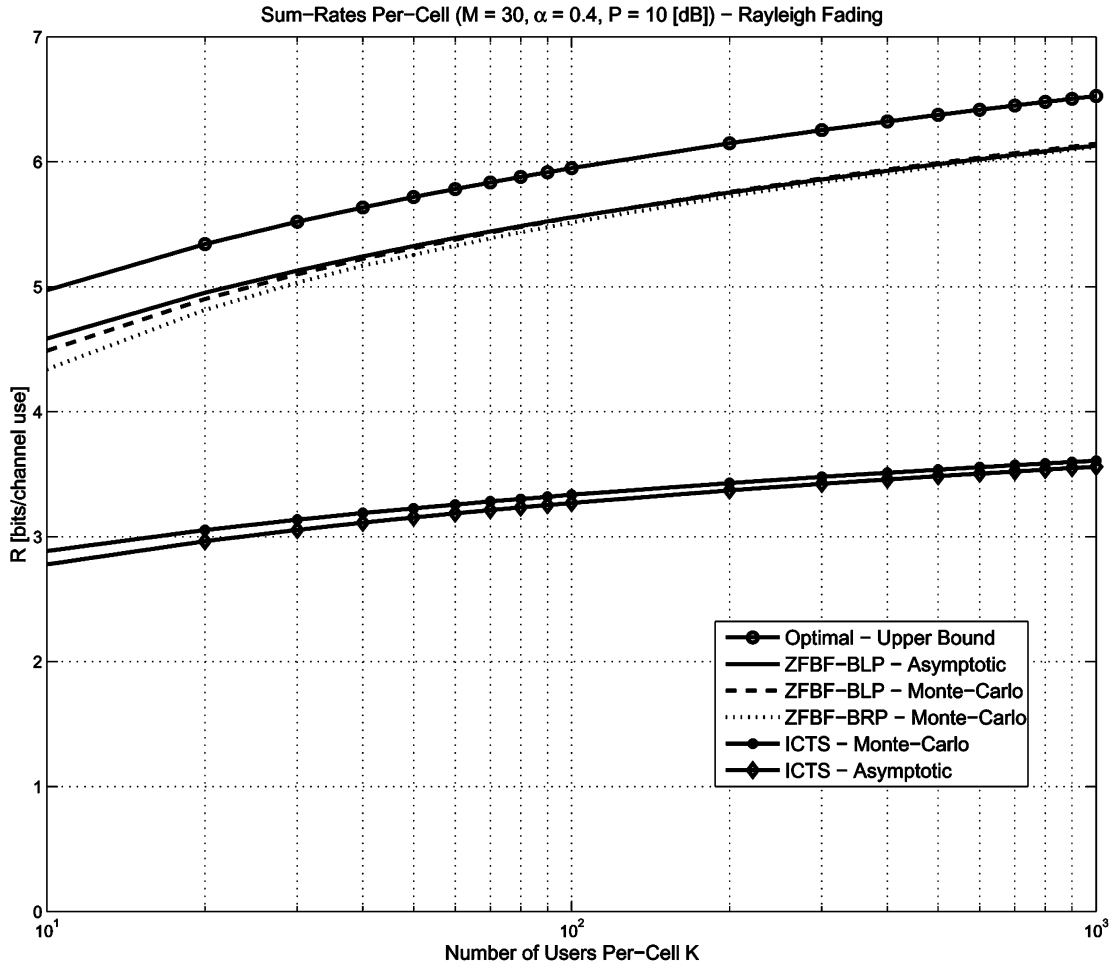


Fig. 5. Sum-rates per cell in the presence of Rayleigh fading versus the number of users per cell K for $P = 10$ [dB], $\alpha = 0.4$, and $M = 30$.

Monte Carlo simulation show a good match to the results predicted by the asymptotic analysis already for a modest number of users. It is noted that since ZFBF is utilized, non-interference-limited behavior is guaranteed for any number of users per cell K (not necessarily large). Moreover, extending the results presented here to a two-dimensional planar Wyner model can be done in a straightforward (though tedious) manner.

A main conclusion of this work is that the simple cooperative multicell ZFBF-BLP scheme presented here provides near-optimal performance already for a moderate number of users per cell. Moreover, the scheduling mechanism prescribes one active user per cell (a natural choice for cellular systems), while treating the whole system as a distributed antenna array for inter-cell interference cancellation by ZFBF (allowing the use of single-user encoding-decoding schemes). Combined with its inherent non-interference-limited behavior, the ZFBF-BLP scheme provides a fair alternative to the optimal complex joint multicell DPC scheme.

APPENDIX

A. Proof of Proposition 2

To prove the right-hand side (RHS) of (8) we note that P_m (expression (7)) satisfies the following set of inequalities:

$$P_m = \frac{MP [(\mathbf{H}\mathbf{H}^\dagger)^{-1}]_{m,m}}{\text{tr}((\mathbf{H}\mathbf{H}^\dagger)^{-1})} \leq P \left(\max_n [(\mathbf{H}\mathbf{H}^\dagger)^{-1}]_{n,n} \right) \left(\max_n \lambda_n(\mathbf{H}\mathbf{H}^\dagger) \right) \stackrel{(a)}{\leq} P \left(\max_n \lambda_n((\mathbf{H}\mathbf{H}^\dagger)^{-1}) \right) \left(\max_n \lambda_n(\mathbf{H}\mathbf{H}^\dagger) \right) = P \frac{\max_n \lambda_n(\mathbf{H}\mathbf{H}^\dagger)}{\min_n \lambda_n(\mathbf{H}\mathbf{H}^\dagger)} \quad (28)$$

where (a) is achieved by recalling that the eigenvalues of an Hermitian matrix majorize its diagonal entries (Horn's theorem [26]).

Next, we denote the nonincreasing ordered eigenvalues and nonincreasing ordered diagonal entries of a semi-positive definite (SPD) Hermitian $M \times M$ matrix \mathbf{A} by $\{\lambda_n^o(\mathbf{A})\}_{n=0}^{M-1}$ and $\{d_n^o(\mathbf{A})\}_{n=0}^{M-1}$, respectively. Now to complete the proof, the RHS of (8) is justified by the following set of inequalities:

$$P_m = \frac{MP [(\mathbf{H}\mathbf{H}^\dagger)^{-1}]_{m,m}}{\text{tr}((\mathbf{H}\mathbf{H}^\dagger)^{-1})} \geq \left(\min_n [(\mathbf{H}\mathbf{H}^\dagger)^{-1}]_{n,n} \right) \left(\min_n \lambda_n(\mathbf{H}\mathbf{H}^\dagger) \right) = P \left[\lambda_{M-1}^o((\mathbf{H}\mathbf{H}^\dagger)^{-1}) + \sum_{n=0}^{M-2} (\lambda_n^o((\mathbf{H}\mathbf{H}^\dagger)^{-1}) - d_n^o((\mathbf{H}\mathbf{H}^\dagger)^{-1})) \right] \times \left(\min_n \lambda_n(\mathbf{H}\mathbf{H}^\dagger) \right)$$

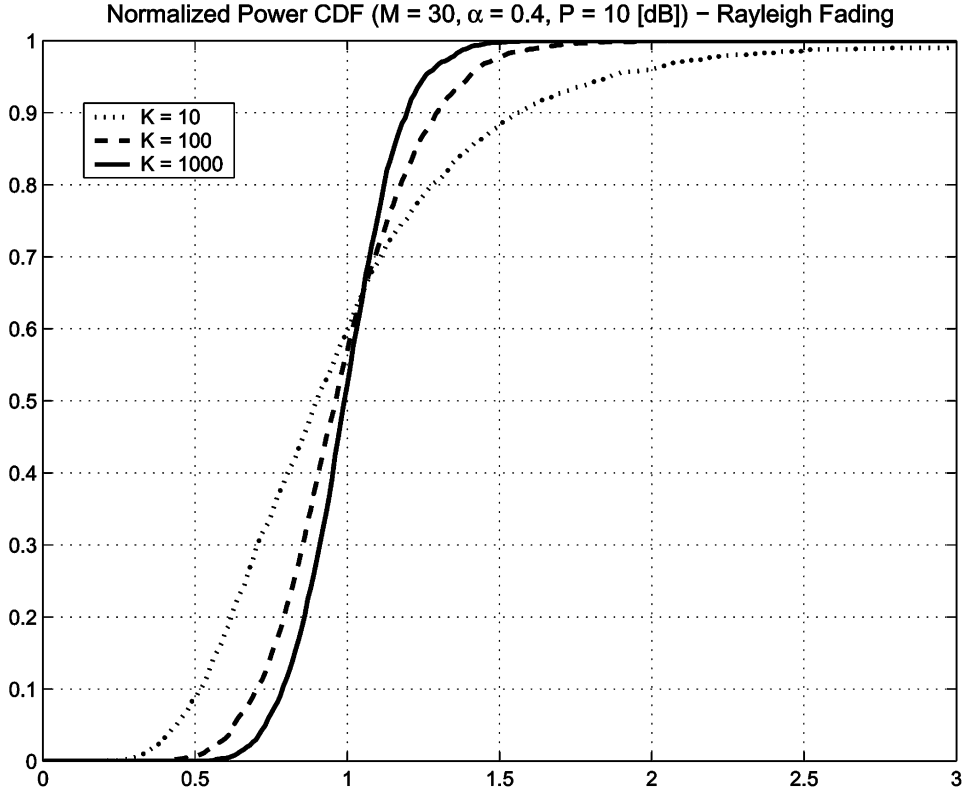


Fig. 6. Normalized transmitted power CDF of an arbitrary base-station in the presence of Rayleigh fading for $P = 10$ [dB], $\alpha = 0.4$, $M = 30$, and several values of K .

$$\begin{aligned} & \stackrel{(a)}{\geq} P (\lambda_{M-1}^o((\mathbf{H}\mathbf{H}^\dagger)^{-1})) \left(\min_n \lambda_n(\mathbf{H}\mathbf{H}^\dagger) \right) & = (1 - 4\alpha^2)^{\frac{3}{2}} & (32) \\ & = P \frac{\min_n \lambda_n(\mathbf{H}\mathbf{H}^\dagger)}{\max_n \lambda_n(\mathbf{H}\mathbf{H}^\dagger)} & (29) \end{aligned}$$

where (a) is achieved by recalling that the eigenvalues of an Hermitian matrix majorize its diagonal entries (Horn's theorem [26]). Hence, the summation term in the second equality of (29) is nonnegative.

B. Proof of Proposition 3

Since for the nonfading setup \mathbf{H} is deterministic, (5) reduces to

$$R_{\text{zfbf-nf}} = \log \left(1 + \frac{MP}{\text{tr}((\mathbf{H}\mathbf{H}^\dagger)^{-1})} \right). \quad (30)$$

To evaluate (30), the following set of equalities are useful:

$$\begin{aligned} \frac{1}{M} \text{tr}((\mathbf{H}\mathbf{H}^\dagger)^{-1}) & \stackrel{(a)}{=} \frac{1}{M} \sum_{m=0}^{M-1} \frac{1}{\lambda_m^2(\mathbf{H})} \\ & = \frac{1}{M} \sum_{m=0}^{M-1} \left(\frac{1}{1 + 2\alpha \cos\left(\frac{2\pi m}{M}\right)} \right)^2 & (31) \end{aligned}$$

where (a) is achieved since \mathbf{H} is an Hermitian nonsingular $M \times M$ matrix for $0 \leq \alpha < 1/2$, and the last equality is due to the fact that \mathbf{H} is also circulant [20]. Taking M to infinity yields

$$\frac{1}{M} \text{tr}((\mathbf{H}\mathbf{H}^\dagger)^{-1}) \underset{M \rightarrow \infty}{=} \int_0^1 (1 + 2\alpha \cos(2\pi\theta))^{-2} d\theta$$

where the last equality is achieved by setting $a = 1$, $b = 2\alpha$, $n = 2$ in [27, eq. 3.661.4, p. 399] and some algebra. Substituting (32) into (30) yields (18).

Since for the nonfading setup \mathbf{H} is a circulant matrix, then according to [20] $(\mathbf{H}\mathbf{H}^\dagger)^{-1}$ is also circulant, and its diagonal entries are equal by definition. Hence, the average transmit power of the m th cell site antenna is given by

$$P_m = [\mathbf{B}\mathbf{B}^\dagger]_{m,m} = \frac{MP [(\mathbf{H}\mathbf{H}^\dagger)^{-1}]_{m,m}}{\text{tr}((\mathbf{H}\mathbf{H}^\dagger)^{-1})} = P \quad (33)$$

where \mathbf{B} is the beamforming matrix defined in (3). It is concluded that the overall power constraint of MP ensures an equal per-cell power constraints of P .

C. Proof of Proposition 4

We start by showing that the channel transfer matrix \mathbf{H} , resulting from the BLP selection procedure, satisfies the following propositions.

Proposition 7: The normalized Frobenius norm of the matrix $(\mathbf{H}\mathbf{H}^\dagger / \log K - \mathbf{I}_M)$ converges in probability to 0. Hence

$$\frac{1}{M} \|\mathbf{H}\mathbf{H}^\dagger / \log K - \mathbf{I}_M\|_F \xrightarrow{P} 0 \quad (34)$$

where $\|\cdot\|_F$ is the Frobenius norm of a matrix.

Proof: See Appendix E. \square

Proposition 8: The eigenvalues of the matrix $(\mathbf{H}\mathbf{H}^\dagger/\log K)$ converge in probability to 1. Hence

$$\lambda_m(\mathbf{H}\mathbf{H}^\dagger)/\log K \xrightarrow{K \rightarrow \infty} 1, \quad \forall m. \quad (35)$$

Proof: See Appendix F. \square

Now, let us define the following event:

$$\mathcal{A} = \{|\lambda_m/\log K - 1| < \epsilon, \forall m\} \quad (36)$$

where λ_m is the m th eigenvalue of $(\mathbf{H}\mathbf{H}^\dagger)$. Next, we apply the high-load slope definition (14) to the per-cell sum-rate (5) and write the following set of inequalities:

$$\begin{aligned} \frac{R_{\text{blp}}}{\log \log K} &= E \left\{ \log \left(1 + \frac{MP}{\sum_m \frac{1}{\lambda_m}} \right) \right\} / \log \log K \\ &\geq E \left\{ \mathbf{1}_{\mathcal{A}} \log \left(1 + \frac{MP}{\sum_m \frac{1}{\lambda_m}} \right) \right\} / \log \log K \\ &\stackrel{(a)}{\geq} \Pr(\mathcal{A}) \frac{\log(1 + (1 - \epsilon)P \log K)}{\log \log K} \\ &\stackrel{(b)}{\geq} \left(\sum_m \Pr \left(\left| \frac{\lambda_m}{\log K} - 1 \right| < \epsilon \right) - (M - 1) \right) \\ &\quad \times \frac{\log(1 + (1 - \epsilon)P \log K)}{\log \log K} \xrightarrow{K \rightarrow \infty} 1 \end{aligned} \quad (37)$$

where $\mathbf{1}_{\mathcal{A}}$ is the indicator function, $\epsilon > 0$ is an arbitrary small constant, (a) is achieved by noting that the definition of \mathcal{A} implies that $\lambda_m > (1 - \epsilon) \log K$, and (b) is achieved by using the following inequality:⁸

$$\Pr \left(\bigcap_{n=1}^N \mathcal{B}_n \right) \geq \sum_{n=1}^N \Pr(\mathcal{B}_n) - (N - 1) \quad (38)$$

where $\{\mathcal{B}_n\}_{n=1}^N$ is a set of arbitrary events. In addition, the final limit of (37) is achieved by invoking Proposition 8 and taking K to infinity.

Since this suboptimal scheme achieves the optimal high-load slope $\mathcal{S}_{\infty}^{\text{blp}} \geq 1$ it is evident that $\mathcal{S}_{\infty}^{\text{blp}} = 1$. Nevertheless, we show that $\mathcal{S}_{\infty}^{\text{blp}} \leq 1$ for the sake of completeness and for later use (i.e., calculating the high-load offset $\mathcal{L}_{\infty}^{\text{blp}}$). Towards this end, the following bound is useful:

$$\begin{aligned} R_{\text{blp}} &\stackrel{(a)}{\leq} \log \left(1 + \frac{P}{M} \sum_m E \left\{ |a_m|^2 + \alpha^2(|b_m|^2 + |c_m|^2) \right\} \right) \\ &\stackrel{(b)}{\leq} \log(1 + P(\log(2K + 1) + 2\alpha^2)) \end{aligned} \quad (39)$$

where (a) is due to Proposition 1, and (b) is achieved due to the fact that according to the BLP selection procedure $|b_m|^2$,

⁸This inequality is a simple generalization of the following inequality: $\Pr(\mathcal{A} \cap \mathcal{B}) \geq \Pr(\mathcal{A}) + \Pr(\mathcal{B}) - 1$ which is valid for any two events \mathcal{A} and \mathcal{B} .

$|c_m|^2 \sim \chi_2^2$ with $E\{|b_m|^2\} = E\{|c_m|^2\} = 1$, and by the fact that the mean value of the r th-order statistic of n independent exponential (or central χ_2^2 with $\sigma^2 = 1/2$) distributed r.v.'s (see [24, p. 62]) satisfies

$$E\{X_{r:n}\} \leq \log \frac{n + \frac{1}{2}}{n - r + \frac{1}{2}}. \quad (40)$$

Applying the upper bound of (39), it is easily verified that the high-load slope of the ZFBF-BLP scheme is upper-bounded by

$$\mathcal{S}_{\infty}^{\text{blp}} \leq \lim_{K \rightarrow \infty} \frac{\log(1 + P(\log(2K + 1) + 2\alpha^2))}{\log \log K} = 1. \quad (41)$$

Turning to the high-load offset, we apply the high-load slope definition (15) to the per-cell sum-rate (5) and write the following set of inequalities:

$$\begin{aligned} \frac{R_{\text{blp}}}{\mathcal{S}_{\infty}^{\text{blp}}} - \log \log K &= E \left\{ \log \left(\frac{1}{\log K} + \frac{MP}{\sum_m \frac{\log K}{\lambda_m}} \right) \right\} \\ &\geq E \left\{ \mathbf{1}_{\mathcal{A}} \log \left(\frac{1}{\log K} + \frac{MP}{\sum_m \frac{\log K}{\lambda_m}} \right) \right\} \\ &\stackrel{(a)}{\geq} \Pr(\mathcal{A}) \log \left(\frac{1}{\log K} + (1 - \epsilon)P \right) \\ &\stackrel{(b)}{\geq} \left(\sum_m \Pr \left(\left| \frac{\lambda_m}{\log K} - 1 \right| < \epsilon \right) - (M - 1) \right) \\ &\quad \times \log \left(\frac{1}{\log K} + (1 - \epsilon)P \right) \\ &\xrightarrow{K \rightarrow \infty} \log((1 - \epsilon)P) \end{aligned} \quad (42)$$

where (a) is due to the definition of \mathcal{A} which implies that $\lambda_m > (1 - \epsilon) \log K$, and (b) is due to (38). The final limit of (42) is achieved by invoking Proposition 8 and taking K to infinity.

Since the high-load lower bound of (42) holds for arbitrary small ϵ it is concluded that

$$\mathcal{L}_{\infty}^{\text{blp}} \geq \log P. \quad (43)$$

On the other hand, applying the upper bound of (39) we get that

$$\begin{aligned} \mathcal{L}_{\infty}^{\text{blp}} &\leq \lim_{K \rightarrow \infty} \log \left(\frac{1}{\log K} + P \frac{(\log(2K + 1) + 2\alpha^2)}{\log K} \right) \\ &= \log P. \end{aligned} \quad (44)$$

Combining (43) and (44) the proof is completed.

D. Proof of Proposition 5

To prove the claim, it is enough to show that the random variables $\{P_m\}_{m=0}^{M-1}$ satisfy

$$\Pr(|P_m - P| \leq \epsilon) \xrightarrow{K \rightarrow \infty} 1, \quad \forall m \quad (45)$$

for any arbitrarily small $\epsilon > 0$.

Now, let us define $\bar{\lambda} \triangleq \max_n \lambda_n(\mathbf{H}\mathbf{H}^\dagger)/\log K$, $\underline{\lambda} \triangleq \min_n \lambda_n(\mathbf{H}\mathbf{H}^\dagger)/\log K$, and rewrite (45) as follows:

$$\begin{aligned}
& \Pr(|P_m - P| \leq \epsilon) \\
&= \Pr\left(\frac{P_m}{P} \leq 1 + \frac{\epsilon}{P} \cap \frac{P_m}{P} \geq 1 - \frac{\epsilon}{P}\right) \\
&\stackrel{(a)}{\geq} \Pr\left(\frac{\bar{\lambda}}{\underline{\lambda}} \leq 1 + \frac{\epsilon}{P} \cap \frac{\underline{\lambda}}{\bar{\lambda}} \leq 1 + \frac{\epsilon}{P}\right) \\
&\stackrel{(b)}{\geq} \Pr\left(\frac{\bar{\lambda}}{\underline{\lambda}} \leq 1 + \frac{\epsilon}{P} \cap \frac{\underline{\lambda}}{\bar{\lambda}} \geq 1 - \frac{\epsilon}{P} \cap |\bar{\lambda} - 1| < \epsilon_1 \right. \\
&\quad \left. \cap |\underline{\lambda} - 1| < \epsilon_2\right) \\
&\stackrel{(c)}{\geq} \Pr\left(\frac{1 + \epsilon_1}{1 - \epsilon_1} \leq 1 + \frac{\epsilon}{P} \cap \frac{1 - \epsilon_2}{1 + \epsilon_2} \geq 1 - \frac{\epsilon}{P} \right. \\
&\quad \left. \cap |\bar{\lambda} - 1| < \epsilon_1 \cap |\underline{\lambda} - 1| < \epsilon_2\right) \\
&\stackrel{(d)}{\stackrel{=}{\geq}} \Pr(|\bar{\lambda} - 1| < \epsilon_1 \cap |\underline{\lambda} - 1| < \epsilon_2) \\
&\stackrel{(e)}{\geq} \Pr(|\bar{\lambda} - 1| < \epsilon_1) + \Pr(|\underline{\lambda} - 1| < \epsilon_2) - 1 \\
&\xrightarrow{K \rightarrow \infty} 1 \tag{46}
\end{aligned}$$

where (a) is due to (8), (b) is due to the fact that $\Pr(\mathcal{A}) \geq \Pr(\mathcal{A} \cap \mathcal{B})$ where \mathcal{A}, \mathcal{B} are arbitrary events, (c) is achieved by increasing $\bar{\lambda}/\underline{\lambda}$ and decreasing $\underline{\lambda}/\bar{\lambda}$, (d) is achieved by setting $\epsilon_1 < \epsilon/(2P + \epsilon)$ and $\epsilon_2 < \epsilon/(2P - \epsilon)$ (i.e., ensuring that the first two events have probability 1), and (e) is achieved by invoking (38) (setting $N = 2$). Finally, the last limit is due to Proposition 8.

E. Proof of Proposition 7

To prove the claim we have to show that

$$\Pr\left(\frac{1}{M} \|\mathbf{H}\mathbf{H}^\dagger/\log K - \mathbf{I}_M\|_F > \epsilon\right) \xrightarrow{K \rightarrow \infty} 0. \tag{47}$$

Using the definition of the Frobenius norm [20], the left-hand side (LHS) of (47) is rewritten as

$$\begin{aligned}
& \Pr\left(\frac{1}{M^2} \sum_{m=0}^{M-1} \sum_{n=0}^{M-1} \left|[\mathbf{H}\mathbf{H}^\dagger/\log K - \mathbf{I}_M]_{m,n}\right|^2 > \epsilon^2\right) \\
&\leq \sum_{m=0}^{M-1} \sum_{n=0}^{M-1} \Pr\left(\left|[\mathbf{H}\mathbf{H}^\dagger/\log K - \mathbf{I}_M]_{m,n}\right|^2 > \frac{M\epsilon^2}{5}\right) \tag{48}
\end{aligned}$$

where the last inequality is achieved by recalling that for any set of nonnegative r.v.'s, $\{x_n\}_{n=1}^N$, the following inequality holds:

$$\Pr\left(\sum_{n=1}^N x_n > \delta\right) \leq \sum_{n=1}^N \Pr(x_n > \delta/N), \tag{49}$$

and that the matrix $\mathbf{H}\mathbf{H}^\dagger$ has $5M$ nonzero entries.

Examining the five-diagonal matrix $\mathbf{H}\mathbf{H}^\dagger$, resulting from the BLP scheduling, reveals that its nonzero entries can be divided into three groups of identical distributed r.v.'s: 1) the main diagonal entries indexed (m, m) ; 2) the entries of the first diagonals below and above the main diagonal, indexed $(m, m \pm 1)$; and 3) the entries of the second diagonals below and above the main

diagonal, indexed $(m, m \pm 2)$. Hence, the RHS of (48) reduces to

$$\begin{aligned}
& M\Pr\left(\left|\frac{|a_m|^2 + \alpha^2 |b_m|^2 + \alpha^2 |c_m|^2}{\log K} - 1\right|^2 > \frac{M\epsilon^2}{5}\right) \\
&+ 2M\Pr\left(\left|\frac{\alpha b_m a_{m-1}^* + \alpha a_m c_{m-1}^*}{\log K}\right|^2 > \frac{M\epsilon^2}{5}\right) \\
&+ 2M\Pr\left(\left|\frac{\alpha^2 b_m c_{m-2}^*}{\log K}\right|^2 > \frac{M\epsilon^2}{5}\right) \tag{50}
\end{aligned}$$

where for Rayleigh fading $b_m, c_m, c_{m-2}, c_{m-1} \sim \mathcal{CN}(0, 1)$, while a_m, a_{m-1} each has the maximum amplitude of K i.i.d. χ_2^2 distributed r.v.'s.

In the sequel, the following order statistic result is useful. According to [23 (Example 1, Appendix A)], the maximum of N χ_2^2 distributed r.v.'s, x , behaves like $\log N$ with high probability. In particular, while neglecting little orders of $\log \log N$, x satisfies

$$\Pr(|x - \log N| \leq \log \log N) > 1 - O\left(\frac{1}{\log N}\right). \tag{51}$$

Next, we denote $d \triangleq \alpha^2(|b_m|^2 + |c_m|^2)$ and rewrite the first summand of (50) as follows:

$$\begin{aligned}
& \Pr\left(\left|\frac{|a_m|^2 + d}{\log K} - 1\right|^2 > \frac{M\epsilon^2}{5}\right) \\
&\stackrel{(a)}{\leq} \Pr\left(\left||a_m|^2 - \log K\right| + d > \frac{\epsilon\sqrt{M} \log K}{\sqrt{5}}\right) \\
&\stackrel{(b)}{\leq} \Pr\left(\left(\left||a_m|^2 - \log K\right| + d\right) > \frac{\epsilon\sqrt{M} \log K}{\sqrt{5}} \right. \\
&\quad \left. \cap \left||a_m|^2 - \log K\right| \leq \log \log K\right) + O\left(\frac{1}{\log K}\right) \\
&\leq \Pr\left(\log \log K + d > \frac{\epsilon\sqrt{M} \log K}{\sqrt{5}}\right) + O\left(\frac{1}{\log K}\right) \\
&\stackrel{(c)}{\stackrel{=}{\leq}} e^{-g_1(\epsilon, K, M, \alpha)}(1 + g_1(\epsilon, K, M, \alpha)) + O\left(\frac{1}{\log K}\right) \\
&\xrightarrow{K \rightarrow \infty} 0 \tag{52}
\end{aligned}$$

where

$$g_1(\epsilon, K, M, \alpha) \triangleq \frac{1}{\alpha^2} \left(\frac{\epsilon\sqrt{M} \log K}{\sqrt{5}} - \log \log K\right) \xrightarrow{K \rightarrow \infty} \infty, \tag{53}$$

(a) is achieved by algebraic manipulation and by invoking the triangular inequality, (b) is due to the fact that $\Pr(\mathcal{A}) \leq \Pr(\mathcal{A} \cap \mathcal{B}) + \Pr(\mathcal{B}^c)$ for any events \mathcal{A}, \mathcal{B} , and by noting that (51) implies that $\Pr(|a_m|^2 - \log K| > \log \log K) < O(1/\log K)$, and (c) is due to the fact that d/α^2 is a χ_4^2 distributed r.v.

Turning to the second summand of (50) we have

$$\Pr\left(\left|\frac{\alpha b_m a_{m-1}^* + \alpha a_m c_{m-1}^*}{\log K}\right|^2 > \frac{M\epsilon^2}{5}\right)$$

$$\leq \Pr \left(\max(|a_{\widehat{m-1}}|^2, |a_m|^2) \frac{(|b_m| + |c_{\widehat{m-1}}|)^2}{(\log K)^2} > \frac{M\epsilon^2}{5\alpha^2} \right) \quad (54)$$

where the last inequality is achieved by invoking the triangular inequality and some algebraic manipulations. Let us define $d \triangleq \max(|a_{\widehat{m-1}}|^2, |a_m|^2)$ and $f \triangleq (|b_m| + |c_{\widehat{m-1}}|)^2$ and rewrite the RHS of (54) as follows:

$$\begin{aligned} & \Pr \left(d f > \frac{\epsilon^2 M (\log K)^2}{5\alpha^2} \right) \\ & \stackrel{(a)}{\leq} \Pr \left(d f > \frac{\epsilon^2 M (\log K)^2}{5\alpha^2} \right. \\ & \quad \left. \cap |d - \log(2K)| < \log \log(2K) \right) + O \left(\frac{1}{\log(2K)} \right) \\ & \leq \Pr \left(f > \frac{\epsilon^2 M (\log K)^2}{5\alpha^2 (\log(2K) + \log \log(2K))} \right) + O \left(\frac{1}{\log(2K)} \right) \\ & \stackrel{(c)}{\leq} \Pr \left(|c_{\widehat{m-1}}|^2 > g_2(\epsilon, K, M, \alpha) \right) \\ & \quad + \Pr \left(|b_m|^2 > g_2(\epsilon, K, M, \alpha) \right) + O \left(\frac{1}{\log(2K)} \right) \\ & \stackrel{(d)}{=} 2e^{-g_2(\epsilon, K, M, \alpha)} + O \left(\frac{1}{\log(2K)} \right) \xrightarrow{K \rightarrow \infty} 0, \quad (55) \end{aligned}$$

where

$$g_2(\epsilon, K, M, \alpha) \triangleq \frac{\epsilon^2 M (\log K)^2}{20\alpha^2 (\log(2K) + \log \log(2K))} \xrightarrow{K \rightarrow \infty} \infty, \quad (56)$$

(a) is achieved by noting that d is the maximum of $2K$ i.i.d. χ_2^2 distributed r.v.'s, and adhering to similar argumentation used in step (b) of (52), (c) is achieved by using (49) and some algebra, and (d) is due to the fact that $|c_{\widehat{m-1}}|^2$ and $|b_m|^2$ are χ_2^2 distributed r.v.'s.

To complete the proof, we consider the third summand of (50) and get

$$\begin{aligned} & \Pr \left(\left| \frac{\alpha^2 b_m c_{\widehat{m-2}}^*}{\log K} \right|^2 > \frac{M\epsilon^2}{5} \right) \\ & \stackrel{(a)}{\leq} \Pr \left(|b_m|^2 + |c_{\widehat{m-2}}|^2 > \frac{2\epsilon\sqrt{M} \log K}{\sqrt{5}\alpha^2} \right) \\ & \stackrel{(b)}{\leq} e^{-g_3(\epsilon, K, M, \alpha)} (1 + g_3(\epsilon, K, M, \alpha)) \xrightarrow{K \rightarrow \infty} 0 \quad (57) \end{aligned}$$

where

$$g_3(\epsilon, K, M, \alpha) \triangleq \frac{2\epsilon\sqrt{M} \log K}{\sqrt{5}\alpha^2} \xrightarrow{K \rightarrow \infty} \infty, \quad (58)$$

(a) is achieved by recalling that for any two nonnegative r.v.'s x, y , the following inequality holds: $\Pr(xy > \delta) \leq \Pr(x + y > 2\sqrt{\delta})$, and (b) is due to the fact that $|b_m|^2 + |c_{\widehat{m-2}}|^2$ is a χ_4^2 distributed r.v.

Remarks: Examining (50), (52), and (55), it is evident that in order for the Frobenius norm to converge we need that $M = o(\log K)$. This requirement that connects the number of cells

M to the number of users per cell K is most unwanted, since it means that a large number of users per cell is needed already for a small number of cells. Fortunately, this requirement evolves from the upper-bounding technique being used (49), and it is not inherent to the performance of the scheme at hand. In fact, numerical results derived by Monte Carlo simulation (see Section VII), reveal that the per-cell sum-rate demonstrates an almost perfect match to its asymptotic expression and also a weak dependency on the number of cells M already for a modest number of users per cell K . The problem with using (49) is that the three terms in (50) are multiplied by M . Hence, $\log K$ must "overcome" M to take the total sum to zero (i.e., $M = o(\log K)$). Despite considerable efforts, we could not show this fact analytically.

F. Proof of Proposition 8

Since the Frobenius norm of an arbitrary rectangular $M \times M$ Hermitian matrix \mathbf{A} may be expressed as

$$\|\mathbf{A}\|_F = \sqrt{\text{tr}(\mathbf{A}^\dagger \mathbf{A})} = \sqrt{\sum_{m=0}^{M-1} \lambda_m^2(\mathbf{A})} \quad (59)$$

then according to Proposition 7, for any finite M we get

$$\begin{aligned} \frac{1}{M} \left\| \frac{\mathbf{H}\mathbf{H}^\dagger}{\log K} - \mathbf{I}_M \right\|_F &= \sqrt{\frac{1}{M^2} \sum_{m=0}^{M-1} \lambda_m^2 \left(\frac{\mathbf{H}\mathbf{H}^\dagger}{\log K} - \mathbf{I}_M \right)} \\ &= \sqrt{\frac{1}{M^2} \sum_{m=0}^{M-1} \left(\frac{\lambda_m(\mathbf{H}\mathbf{H}^\dagger)}{\log K} - 1 \right)^2} \\ &\xrightarrow{K \rightarrow \infty} 0 \quad (60) \end{aligned}$$

and the proof is completed by noting that the last equality of (60) holds if and only if (35) holds.

G. Proof of Proposition 6

To assess the high-load characterization parameters of the ZFBF-BRP scheme, the following bound is useful:

$$\begin{aligned} R_{\text{brp}} &= E \left\{ \log \left(1 + \frac{MP}{\text{tr}(\mathbf{H}\mathbf{H}^\dagger - 1)} \right) \right\} \\ &\stackrel{(a)}{\leq} \log \left(1 + \frac{P}{M} E \{ \text{tr}(\mathbf{H}\mathbf{H}^\dagger) \} \right) \\ &\leq \log \left(1 + \frac{P}{M} \sum_m E \{ [\mathbf{H}\mathbf{H}^\dagger]_{m,m} |_{\alpha=1} \} \right) \\ &= \log \left(1 + \frac{P}{M} \sum_m E \{ |d_m|^2 \} \right) \quad (61) \end{aligned}$$

where (a) is due to Proposition 1, and $|d_m|^2 \triangleq |a_m|^2 + |b_m|^2 + |c_m|^2$. It is noted that $|d_m|^2$ is the maximum of K i.i.d. χ_6^2 distributed r.v.'s with $\sigma^2 = 1/2$. Next we upper-bound $E \{ |d_m|^2 \}$, utilizing order statistics argumentations.

Proposition 9: The mean value of the r th ($1 \leq r \leq n$)-order statistics of a central χ_{2l}^2 distribution satisfies

$$E\{X_{r:n}\} \leq 2\sigma^2 \left(\frac{\log\left(\frac{2n+1}{2n-2r+1}\right) + l \log \frac{1}{\beta} + \log l - l}{1 - l\beta} \right) \quad (62)$$

where $0 < \beta < 1/l$.

Proof: See Appendix H. \square

For the current case of interest, i.e., $l = 3$, $\sigma^2 = 1/2$, $r = n$, $n = K$, and $\beta = 1/(3 \log K)$, we get that (62) boils down $\forall m$ to

$$E\{|d_m|^2\} \leq \frac{\log(2K+1) + 3 \log \log K + \log 3 + 3 \log \log 3 - 3}{1 - \frac{1}{\log K}}. \quad (63)$$

Finally, substituting (63) in (61), noting that $\log 3 + 3 \log \log 3 - 3 < 0$, and applying the definitions of the high-load slope and offset, the proof is completed.

H. Proof of Proposition 9

In [24, p. 62], it is shown that the average of the r th-order statistics $\bar{x} = E\{X_{r:n}\}$ of an arbitrary distribution $P(x)$ satisfies the following:

$$P(\bar{x}) \leq \frac{r}{n + \frac{1}{2}} \quad (64)$$

if its *hazard rate*, defined as

$$h(x) \triangleq \frac{\frac{dP(x)}{dx}}{1 - P(x)}, \quad (65)$$

is an increasing function.

It is easily verified that the hazard rate of a central χ_{2l}^2 distribution is an increasing function. Hence, the average of its r th-order statistics satisfies (64). On the other hand, it is easy to verify that the χ_{2l}^2 distribution function also satisfies

$$P(x) \geq 1 - le^{-\frac{x}{2\sigma^2}} \left(\frac{x}{2\sigma^2} \right)^l, \quad x \geq 0. \quad (66)$$

Combining (64) and (66), and some algebra we get the following inequality:

$$\frac{\bar{x}}{2\sigma^2} \leq \log \frac{2n+1}{2n-2r+1} + l \log \frac{\bar{x}}{2\sigma^2} + \log l. \quad (67)$$

Finally, by invoking the following inequality

$$\log y \leq \log \frac{1}{\beta} - 1 + \beta y, \quad y \geq 0, \quad \beta > 0 \quad (68)$$

to the second summand of the LHS of (67) and some algebra the proof is completed.

ACKNOWLEDGMENT

The authors would like to thank Dr. Anelia Somekh-Baruch for helpful discussions, and the Associated Editor Dr. Gerhard Kramer for his constructive comments that greatly improved the quality of this work.

REFERENCES

- [1] S. Shamai (Shitz), O. Somekh, and B. M. Zaidel, "Multi-cell communications: An information theoretic perspective," in *Proc. Joint Workshop on Communications and Coding (JWCC'04)*, Donnini, Florence, Italy, Oct. 2004.
- [2] O. Somekh, O. Simeone, Y. Bar-Ness, A. M. Haimovich, U. Spagnolini, and S. Shamai (Shitz), *Distributed Antenna Systems: Open Architecture for Future Wireless Communications*. Boca Raton, FL: Auerbach Publications, CRC, 2007, ch. An Information Theoretic View of Distributed Antenna Processing in Cellular Systems.
- [3] G. Foschini, H. C. Huang, K. Karakayali, R. A. Valenzuela, and S. Venkatesan, "The value of coherent base station coordination," in *Proc. 2005 Conf. Information Sciences and Systems (CISS'05)*, Baltimore, MD, Mar. 18, 2005.
- [4] H. Zhang, H. Dai, and Q. Zhou, "Base station cooperation for multiuser MIMO: Joint transmission and BS selection," in *Proc. 2004 Conf. Information Sciences and Systems (CISS'04)*, Princeton, NJ, Mar. 2004.
- [5] A. Ekbal and J. M. Cioffi, "Distributed transmit beamforming in cellular networks," in *Proc. ICC 2005 Wireless Communications Theory (ICC'05)*, Seoul, Korea, May 2005, vol. 4, pp. 2690–2694.
- [6] A. D. Wyner, "Shannon-theoretic approach to a Gaussian cellular multiple-access channel," *IEEE Trans. Inf. Theory*, vol. 40, no. 6, pp. 1713–1727, Nov. 1994.
- [7] S. Shamai (Shitz) and B. M. Zaidel, "Enhancing the cellular downlink capacity via co-processing at the transmitting end," in *Proc. IEEE 53rd Vehicular Technology Conf. (VTC 2001 Spring)*, Rhodes, Greece, May 2001, vol. 3, pp. 1745–1749.
- [8] O. Somekh, B. M. Zaidel, and S. Shamai (Shitz), "Sum rate characterization of joint multiple cell-site processing," *IEEE Trans. Inf. Theory*, vol. 53, no. 12, pp. 4473–4497, Dec. 2007.
- [9] H. Weingarten, Y. Steinberg, and S. Shamai (Shitz), "The capacity region of the Gaussian multiple-input multiple-output broadcast channel," *IEEE Trans. Inf. Theory*, vol. 52, no. 9, pp. 3936–3964, Sep. 2006.
- [10] A. Wiesel, Y. C. Eldar, and S. Shamai (Shitz), "Linear precoding via conic optimization for fixed MIMO receivers," *IEEE Trans. Signal Process.*, vol. 54, no. 1, pp. 161–176, Jan. 2006.
- [11] M. Stojnic, H. Vikalo, and B. Hassibi, "Maximizing the sum-rate of multi-antenna broadcast channels using linear preprocessing," *IEEE Trans. Wireless Commun.*, vol. 5, no. 9, pp. 2338–2342, Sep. 2006.
- [12] W. Yu and T. Lan, "Transmitter optimization for the multi-antenna downlink with per-antenna power constraints," *IEEE Trans. Signal Process.*, vol. 55, no. 6, pp. 2646–2660, Jun. 2007.
- [13] G. Caire and S. Shamai (Shitz), "On the achievable throughput of a multiple-antenna Gaussian broadcast channel," *IEEE Trans. Inf. Theory*, vol. 49, no. 7, pp. 1691–1706, Jul. 2003.
- [14] F. Boccardi and H. Huang, "Optimum power allocation for the MIMO-BC zero-forcing precoder with per-antenna power constraints," in *Proc. 2006 Conf. Information Sciences and Systems (CISS'06)*, Princeton, NJ, Mar. 2006.
- [15] C. B. Chae, R. Heath, and D. Mazzaresse, "Achievable sum-rate bounds of zero-forcing based linear multi-user MIMO systems," in *Proc. 44th Annu. Allerton Conf. Communication, Control and Computing*, Monticello, IL, Sep. 2006.
- [16] J. Jiang, R. Buehrer, and W. Tranter, "Greedy scheduling performance for a zero-forcing dirty-paper coded system," *IEEE Trans. Commun.*, vol. 54, no. 5, pp. 789–793, May 2006.
- [17] T. Yoo and A. Goldsmith, "On the optimality of multi-antenna broadcast scheduling using zero forcing beam forming," *IEEE J. Sel. Areas Commun.*, vol. 24, no. 3, pp. 528–541, Mar. 2006.
- [18] A. Vakili, A. Dana, M. Sharif, and B. Hassibi, "Differentiated rate scheduling for MIMO broadcast channels," in *Proc. 44th Annu. Allerton Conf. Communication, Control, and Computing (Allerton'06)*, Monticello, IL, Sep. 2006.
- [19] A. Lozano, A. Tulino, and S. Verdú, "High-SNR power offset in multi-antenna communications," *IEEE Trans. Inf. Theory*, vol. 51, no. 12, pp. 4134–4151, Dec. 2005.
- [20] R. M. Gray, "On the asymptotic eigenvalue distribution of Toeplitz matrices," *IEEE Trans. Inf. Theory*, vol. IT-18, no. 6, pp. 725–730, Nov. 1972.

- [21] S. Shamai (Shitz) and A. D. Wyner, "Information-theoretic considerations for symmetric, cellular, multiple-access fading channels—Part I," *IEEE Trans. Inf. Theory*, vol. 43, no. 6, pp. 1877–1894, Nov. 1997.
- [22] S. Shamai (Shitz) and S. Verdú, "The impact of frequency-flat fading on the spectral efficiency of CDMA," *IEEE Trans. Inf. Theory*, vol. 47, no. 4, pp. 1302–1327, May 2001.
- [23] M. Sharif and B. Hassibi, "On the capacity of MIMO broadcast channel with partial side information," *IEEE Trans. Inf. Theory*, vol. 51, no. 2, pp. 506–522, Feb. 2005.
- [24] H. A. David, *Order Statistics*. New York: Wiley, 1970.
- [25] W. Choi and J. G. Andrews, "The capacity gain from base station cooperative scheduling in a MIMO DPC cellular system," in *Proc. IEEE Int. Symp. Information Theory (ISIT'06)*, Seattle, WA, Jul. 2006, pp. 1224–1228.
- [26] A. Horn, "Doubly stochastic matrices and the diagonal of a rotation matrix," *Amer. J. Math.*, vol. 76, pp. 620–630, 1954.
- [27] I. S. Gradshteyn and I. M. Ryzhik, *Tables of Integrals, Series, and Products*, 6 ed. San Diego, CA: Academic, 2000.

Oren Somekh (S'90–M'06) received the B.Sc., M.Sc., and Ph.D. degrees in electrical engineering from the Technion–Israel Institute of Technology, Haifa, Israel, in 1989, 1991, and 2005, respectively.

During 1991–1996, he served in the Israel Defense Forces (IDF) in the capacity of a Research Engineer. During 1998–2002, he was the Vice President of Research and Development (VP R&D) and later the Chief Technical Officer (CTO) of Surf Communication Solutions Ltd., Yokneam, Israel. From April 2005 to October 2006, he was a Visiting Research Fellow at the Center for Wireless Communications and Signal Processing Research (CWCSRP), New Jersey Institute of Technology (NJIT), Newark, NJ. Since November 2006, he has been a Visiting Research Fellow in the Electrical Engineering Department of Princeton University, Princeton, NJ. His current main research interest are information-theoretical aspects of cooperative wireless networks.

Dr. Somekh is a recipient of the European Community (EC) Marie Curie Outgoing International Fellowship (OIF), he was the corecipient of the first IEEE Information Theory Society ISIT best student paper award (2007), and the coinventor of several patents in the field of communications.

Oswaldo Simeone (M'02) received the M.Sc. degree (with honors) and the Ph.D. degree in information engineering from Politecnico di Milano, Milan, Italy, in 2001 and 2005 respectively.

He is currently with the Center for Wireless Communications and Signal Processing Research (CWCSRP), at the New Jersey Institute of Technology (NJIT), Newark, NJ, where he is an Assistant Professor. His current research interests concern the cross-layer analysis and design of wireless networks with emphasis on information-theoretic, signal processing, and queuing aspects. Specific topics of interest are: cognitive radio, cooperative communications, *ad hoc*, sensor, mesh, and hybrid networks, distributed estimation, and synchronization.

Prof. Simeone is the corecipient of the best paper awards of IEEE SPAWC 2007 and IEEE WRECOM 2007. He currently serves as an Editor for IEEE TRANSACTIONS ON WIRELESS COMMUNICATIONS.

Yeheskel Bar-Ness (M'69–SM'79–F'89–LF'06) received the B.Sc. and M.Sc. degrees in electrical engineering from the Technion–Israel Institute of Technology, Haifa, Israel, and the Ph.D. degree in applied mathematics from Brown University, Providence, RI.

He is a Distinguished Professor of Electrical and Computer engineering, Foundation Chair of Communication and Signal Processing Research, and Executive Director of the Center for Wireless Communication and Signal Processing Research (CCSPR) at the New Jersey Institute of Technology (NJIT), Newark. After working in the private sector, he joined the School of Engineering, Tel-Aviv University, Tel-Aviv, Israel, in 1973. He came to NJIT from AT&T Bell Laboratories in 1985. Current research interests include design of MIMO-OFDM, and MC-CDMA, adaptive array and spatial interference cancellation and signal separation for multiuser communications, and modulation classification. Recently, he is contributing in the area of cooperative communication, modulation classification, cognitive radio, link adaptation with cooperative diversity, cross-layer design and analysis and scheduling, and beam-forming for downlink with limited feedback. He published numerous papers in these areas.

Prof. Bar-Ness serves on the editorial board of *WIRED Magazine*, was the founding Editor-in-chief of IEEE COMMUNICATION LETTERS, and was Associate and Area Editor for IEEE TRANSACTIONS ON COMMUNICATIONS. He is currently on the editorial board of the *Journal of Communication Networks*. He has been the Technical Chair of several major conferences and symposia and was the recipient of the Kaplan Prize (1973), which is awarded annually by the government of Israel to the ten best technical contributors. He is the recipient of the IEEE Communication Society's "Exemplary Service Award." He was selected the "NJ 2006 Inventor of the Year," for "systems and methods to enhance wireless/mobile communications," and in November 2008, he received the "Thomas Alva Edison Patent Award."

Alexander M. Haimovich (S'82–M'87–SM'97) received the B.Sc. degree in electrical engineering from the Technion–Israel Institute of Technology, Haifa, Israel, in 1977, the M.Sc. degree in electrical engineering from Drexel University, Philadelphia, PA, in 1983, and the Ph.D. degree in systems from the University of Pennsylvania, Philadelphia, in 1989.

He is a Professor of Electrical and Computer Engineering at the New Jersey Institute of Technology, Newark. His research interests include MIMO radar and communication systems, wireless networks, and source localization.

Dr. Haimovich is currently a Guest Editor for the Special Issue on MIMO Radar of the *Journal for Special Topics in Signal Processing*.

Shlomo Shamai (Shitz) (S'80–M'82–SM'88–F'94) received the B.Sc., M.Sc., and Ph.D. degrees in electrical engineering from the Technion–Israel Institute of Technology, Haifa, Israel, in 1975, 1981, and 1986, respectively.

During 1975–1985, he was with the Communications Research Labs in the capacity of a Senior Research Engineer. Since 1986, he has been with the Department of Electrical Engineering, Technion–Israel Institute of Technology, where he is now the William Fondiller Professor of Telecommunications. His research interests encompasses a wide spectrum of topics in information theory and statistical communications.

Dr. Shamai (Shitz) is a member of the Union Radio Scientifique Internationale (URSI). He is the recipient of the 1999 van der Pol Gold Medal of URSI, and a corecipient of the 2000 IEEE Donald G. Fink Prize Paper Award, the 2003 and the 2004 joint IEEE IT/COM Societies Paper Award, and the 2007 IEEE Information Theory Society Paper Award. He is also the recipient of 1985 Alon Grant for distinguished young scientists and the 2000 Technion Henry Taub Prize for Excellence in Research. He has served as Associate Editor for the Shannon Theory of the IEEE TRANSACTIONS ON INFORMATION THEORY, and also has served on the Board of Governors of the IEEE Information Theory Society.